PHYSICAL REVIEW B

CONDENSED MATTER

THIRD SERIES, VOLUME 47, NUMBER 1 1 JANUARY 1993-I

Soft-mode studies in $KTa_{0.93}Nb_{0.07}O_3$ with use of the time-resolved third-order optical susceptibility χ^3

P. Grenier
Département de Physique, Université de Sherbrooke, Sherbrooke, Québec, Canada J1K 2R1

D. Houde
Département de Médecine Nucléaire et de Radiobiologie, Université de Sherbrooke, Sherbrooke, Québec, Canada J1K 2R1

S. Jandl
Département de Physique, Université de Sherbrooke, Sherbrooke, Québec, Canada J1K 2R1

L. A. Boatner
Solid State Division, Oak Ridge National Laboratory, P.O. Box 2008, Oak Ridge, Tennessee 37831-6056
(Received 10 February 1992; revised manuscript received 17 April 1992)

Determinations of the third-order optical susceptibility have been used to investigate the dynamical properties of the A_1(TO) soft-polariton mode in $KTa_{0.93}Nb_{0.07}O_3$ as a function of temperature. Saturation of the soft-polariton frequency as $T \rightarrow T_c$ indicates an interaction with the relaxation mode and evidence is found for the presence of low-frequency excitations that significantly increase the observed damping rate. Also, with the use of the polariton dispersion and self-energy formulas, frequency and damping are compared to the TO Raman-active phonon parameters.

I. INTRODUCTION

The dynamical behavior associated with structural phase transitions is a subject of long-standing interest in solid-state science, and, in particular, the simultaneous existence of quasielastic and phonon features in the dynamic response of such systems has been the subject of a number of theoretical and experimental investigations.[1-6] At the present time, the role played by interactions responsible for the so-called "central peak" phenomena and their associated contributions to the initiation of structural phase transitions in a nominally pure system such as $KNbO_3$ is reasonably well established.[5] In the case of more complex solid-solution, mixed-crystal systems such as $KTa_{1-x}Nb_xO_3$ (KTN), however, the exact role played by the different constituent cations in influencing or determining the dynamics of the phase transition remains a subject of active investigation.[6,7]

The relatively recent development of femtosecond optical lasers has provided a powerful technique for the study of the dynamics of displacive phase transitions which result in the formation of a ferroelectric phase. In particular, the method of impulsive stimulated light scattering utilized by Yan and Nelson[8] represents a general technique for following the time evolution of a dynamic system by employing an initial coherent excitation with pump pulses and a subsequent probing of the time evolution of the system by an additional time-delayed pulse. As recently noted by Etchepare *et al.*,[9] this type of approach may be more appropriate for investigations of the dynamics of phase transitions than its Raman-scattering counterpart, since the resolution of the dynamics is in the time domain rather than the frequency domain where the central-peak and soft-mode contributions merge at $\omega \rightarrow 0$ as $T \rightarrow T_c$. In the present work, the technique of stimulated light scattering is used to investigate the dynamics of the solid-solution system $KTa_{0.93}Nb_{0.07}O_3$ as a function of temperature in the temperature range below the phase transition.

II. THEORETICAL BACKGROUND

The present investigation utilizes a nondegenerate, four-wave-mixing technique that is similar to the approach described previously by Etchepare *et al.*[10] and Thomazeau *et al.*[11] A detailed description of this experimental approach has been presented elsewhere.[8,12,13]

Following the formalism developed by Yan *et al.*,[8] it is possible to relate the diffraction efficiency to the Green's function of the excited modes in the material through the expression

 ©1993 The American Physical Society

$$S(\mathbf{q},t)\sim|G(\mathbf{q},t)|^2\ , \tag{1}$$

where $\mathbf{q}=\mathbf{k}_{p1}-\mathbf{k}_{p2}$ represents the wave-vector transfer related to the exciting geometry, and $\mathbf{k}_{p1,2}$ represent the pump wave vectors. In the present case of a KTN single crystal, the mode of interest is the damped soft mode (or, more precisely, a polariton at a fixed $\mathbf{q}$) and the coupling of this mode to relaxation modes.[1,3,5] The Green's function at fixed $\mathbf{q}$ for a phonon without coupling is given by the expression

$$G_p(\omega)=[\Omega_0^2-\omega^2-2i\omega\gamma_0]^{-1}\ ,$$

where Ω_0 and γ_0 are, respectively, the quasiharmonic frequency and damping of the phonon. The retarded Green's function is then

$$G_p(t)=B\exp(-\gamma_0 t)\sin(\Omega t)\ , \tag{2}$$

where $\Omega=\sqrt{\Omega_0^2-\gamma_0^2}$. In the case of coupled-phonon and quasielastic components, the following phenomenological form for the Green's function is used:[1,4]

$$G_{p\text{-}r}(\omega)=\left[\Omega_0^2-\omega^2-2i\omega\gamma_0+\frac{\omega\eta^2}{(\omega+i\gamma_r)}\right]^{-1}\ , \tag{3}$$

where γ_r is the inverse relaxation time of the Debye relaxation mode, and η is the coupling constant. The retarded Green's function can then be expressed as

$$G_{p\text{-}r}(t)=C\exp(-\tilde{\gamma}_r t)+D\exp(-\tilde{\gamma}t)\sin(\tilde{\Omega}t+\varphi)\ , \tag{4}$$

where the parameters $\tilde{\gamma}_r$, $\tilde{\gamma}$, and $\tilde{\Omega}$ are related to the renormalized poles $\pm\tilde{\Omega}-i\tilde{\gamma}$ and $-i\tilde{\gamma}_r$ of the phonon and relaxation mode, respectively.

The term $C\exp(-\gamma_r t)$ in Eq. (4) is negligible since numerical evaluation with typical values of Ω_0, γ_0, γ_r, and η as found in the literature for perovskyte materials[3,4,5] gives $D/C>200$. Thus, the coupling effect [Eq. (4) compared to Eq. (2)] will mainly manifest itself in a renormalization of the frequency and damping and in the presence of a phase factor in the oscillating term,

$$\varphi=tg^{-1}\left[\frac{\tilde{\gamma}_r-\tilde{\gamma}}{\tilde{\Omega}}\right]-tg^{-1}\left[\frac{\gamma_r-\tilde{\gamma}}{\tilde{\Omega}}\right]\ , \tag{5}$$

which is negative if, as found by calculation, $\tilde{\gamma}_r<\gamma_r$. In order to account for the instantaneous part of the response,[9] a Dirac δ function $\delta(t)$ is added to the Green's function to give the total response function. Consequently, the diffraction efficiency as a function of time delay τ_d between the pump and probe pulse can be expressed as

$$S(\tau_d)=\int dt\left[\int d\tau[A\,\delta(\tau)+B\exp(-\tilde{\gamma}\tau)\sin(\tilde{\Omega}\tau+\varphi)]I_p(t-\tau)\right]^2 I_t(t-\tau_d)\ , \tag{6}$$

where $I_p(t)$ and $I_t(t)$ represent the pump- and probe-pulse profiles, respectively.

III. EXPERIMENTAL

The present investigations were carried out using a single crystal of KTN with the composition $KTa_{0.93}Nb_{0.07}O_3$ and a transition temperature T_c of $\sim$68 K. This crystal, whose dimensions were $0.25\times1.6\times5.0$ mm, was cut along the rhombohedral axes ($a=[2\bar{1}\,\bar{1}]$, $b=[01\bar{1}]$, $c=[111]$). An electric field of $\sim$3.0 kV/cm was applied along the crystal c axis during cooling in order to pole the sample. When the sample had stabilized at a low temperature, the electric field was decreased to 600 V/cm, and the experiment was then performed with this residual field applied. The maintenance of this residual applied field was required during the measurements since the single domain produced by cooling in the 3.0-kV/cm field tended to relax even at temperatures in the range of $T=10$ K. This relaxation resulted in a decrease in the diffracted signal and an accompanying increase in the scattering of the pump pulse.

The experiments were performed using a forward-folded boxcar geometry[11] with two pump pulses at 620 nm and a probe pulse at 650 nm. Both the pump and probe pulses had a temporal width of $\sim$100 fs. The two pump pulses, which made an angle of 2.68° inside the crystal, were incident along the direction of the a axis and were polarized along the c axis. The resulting phonons propagated along the b axis and were of A_1 symmetry. The diffracted signal, which was polarized along the c axis, permitted the measurements of the elements of the $\chi^{(3)}_{cccc}$ susceptibility tensor.

IV. EXPERIMENTAL RESULTS

The observed diffraction efficiency for $KTa_{0.93}Nb_{0.07}O_3$ as a function of the probe-pulse time delay is illustrated in Fig. 1 for various temperatures above and below the transition temperature T_c. As $T\rightarrow T_c$, the frequency decreases while the observed damping increases. For $T>T_c$ (where only the virtual electronic excitations contribute to the time response), the temporal profile of the pulse is observed.

The frequency $\tilde{\Omega}$ and damping $\tilde{\gamma}$ as obtained from a least-squares fit to the data using Eq. (6) are illustrated in Figs. 2 and 3. With the frequency that seems to saturate as $T\rightarrow T_c$, there is an indication of coupling between the soft mode and the relaxation mode. However, the value obtained for φ is $14°\pm8°$, which is opposite in sign to what Eq. (5) predicts. Nevertheless, the existence of this phase points towards some kind of coupling since, without any interaction, there is no phase in the response function of the phonon [Eq. (2)].

As $T\rightarrow T_c$, the observed increase in the damping is relatively high, and such values are not in agreement with the Raman-scattering results,[4,7] where smaller values are usually found. Overestimates of the damping in transient scattering experiments may result from the group veloci-

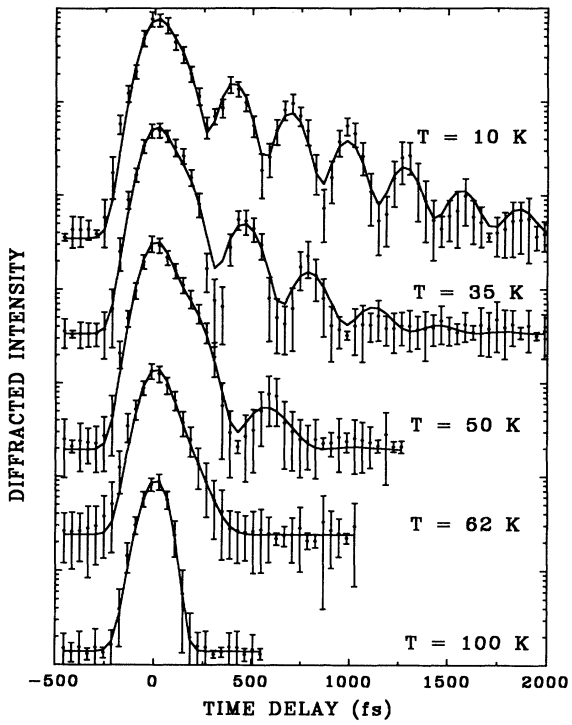

FIG. 1. Intensity of the diffracted signal as a function of the time delay between the pump and probe pulses for different temperatures. The symbols represent the experimental data points, and solid lines are the fit to Eq. (6).

ty of the mode being investigated, since the excitations move away from the point where they are created and where they interact with the probe pulse.[8] The group velocity may be quite high in the case of a polariton[14] (up to $V_g \sim c/\sqrt{\epsilon_0}$). In the present case, however, this should not present a problem since, as $T \rightarrow T_c$, the static dielectric constant increases strongly thereby producing a significant decrease in the group velocity. Accordingly, any contributions of this phenomenon to the damping become negligible as $T \rightarrow T_C$.

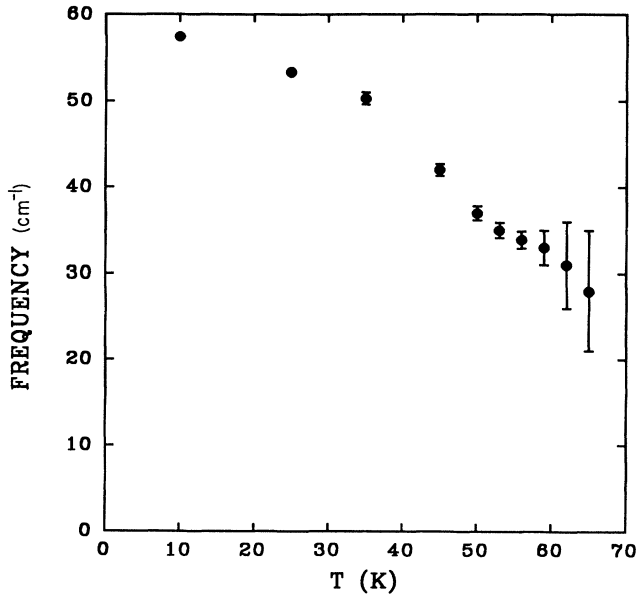

FIG. 2. Values of the frequency ($\tilde{\Omega}$) as a function of temperature obtained by fitting the experimental results.

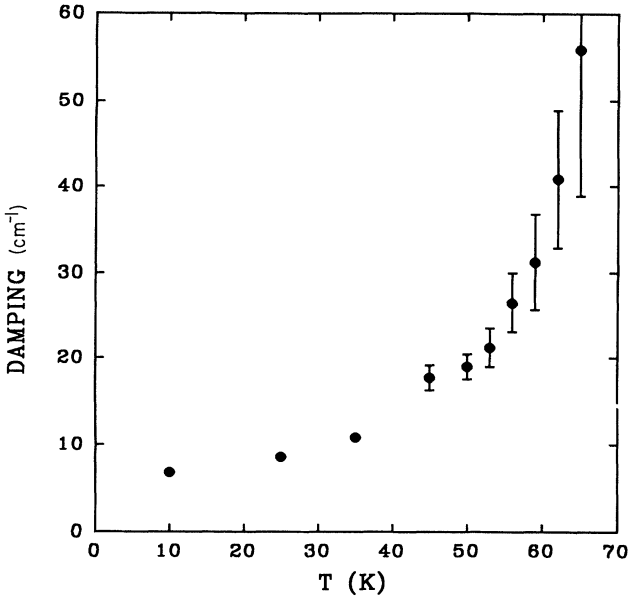

FIG. 3. Values of the damping ($\tilde{\gamma}$) as a function of temperature obtained by fitting the experimental results.

The origin of the discrepancy between the present results and the Raman-scattering measurements may be associated with the polariton since our experiment involves a wave-vector transfer of $cq_{\rm exp}/n = 755\ {\rm cm}^{-1}$ while for right-angle Raman scattering $cq/n \simeq 25\,000\ {\rm cm}^{-1}$ with n standing for the refraction index.

The polariton dispersion relation relates our data to the $\omega_{\rm TO}$ and $\gamma_{\rm TO}$ of the phonon obtained in right-angle configuration Raman scattering. In the following, we will evaluate this dispersion relation with a reasonable assumption of the phonon characteristics. We shall then verify that we can reconcile our measurement with Raman-scattering results if we use a frequency-dependent damping function for the phonon that reaches a maximum at some frequency smaller than $\omega_{\rm TO}$.

For the polariton the response function of Eq. (6) is still valid. However, $\tilde{\Omega}$ and $\tilde{\gamma}$ are replaced by the frequency $\Omega_\pi(q=q_{\rm exp})$ and damping $\gamma_\pi(q=q_{\rm exp})$ of the polariton. According to the Benson and Mills[15] calculation, $\Omega_\pi(q)$ and $\gamma_\pi(q)$ are related to the poles of the following Green's function:

$$G_{p\text{-}p}(q,\omega) = \frac{c^2q^2/n^2-\omega^2}{[\omega^2+2\pi(\omega)-\omega_{\rm TO}^2][\omega^2-c^2q^2/n^2]-S^2\omega^2}\ , \tag{7}$$

where $\pi(\omega)=\Delta(\omega)+i\omega\gamma_{\rm TO}(\omega)$ is the proper self-energy of the phonon, S is the ionic plasma frequency related to the transverse ($\omega_{\rm TO}$) and the longitudinal ($\omega_{\rm LO}$) phonon frequency by the relation $S^2=\omega_{\rm LO}^2-\omega_{\rm TO}^2$.

Results for the numerical evaluation of Eq. (7) in the simple case of a constant-phonon damping

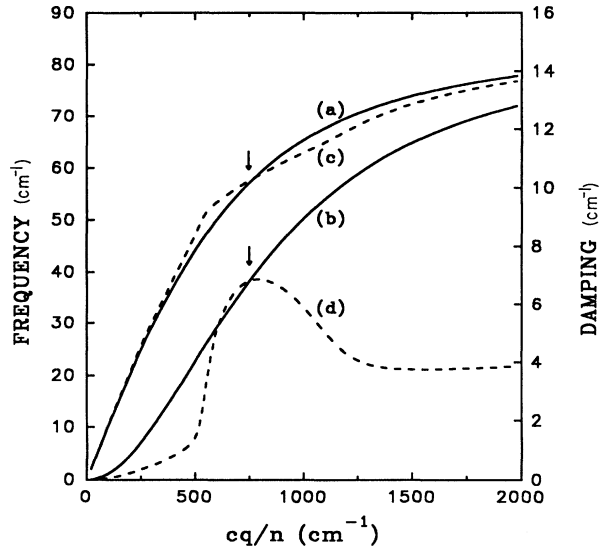

FIG. 4. Polariton dispersion relation obtained from Eq. (7). (a) and (b) Frequency and damping vs cq/n for a constant phonon proper self-energy, (c) and (d) for a phonon proper self-energy given by Eq. (8). Arrows correspond to the experimental wave vector.

$[\gamma_{TO}(\omega)=\gamma_{TO}]$ with $S=820\ \mathrm{cm}^{-1}$ (such a value of S is usually found in these perovskyte materials[16,17]), $\omega_{TO}=85.4\,\mathrm{cm}^{-1}$, and $\gamma_{TO}=15\ \mathrm{cm}^{-1}$ are presented in Figs. 4(a) and 4(b). Only the poles associated with the lower polariton branch have been plotted. ω_{TO} and γ_{TO} are chosen so that $\Omega_\pi(q=q_{exp})$ and $\gamma_\pi(q=q_{exp})$ correspond to $\tilde{\Omega}$ and $\tilde{\gamma}$ measured at $T=10$ K. This model predicts $\gamma_{TO}=2\tilde{\gamma}$.

When a phonon is coupled with some low-lying states such as acoustical phonons, larger values of $\gamma_\pi(q)$ relative to γ_{TO} could be obtained, as observed by Ushioda *et al.*[18,19] in GaP. In this case, the following phenomenological formula is used for the phonon proper self-energy:[20,21]

$$\pi(\omega)=i\omega\gamma_{TO}-\frac{b^2}{[\omega_A^2-\omega^2]-2i\omega\gamma_A}\ . \tag{8}$$

Figures 4(c) and 4(d) present the polariton frequency and damping dependence obtained with this formula, where $S=820\,\mathrm{cm}^{-1}$, $\omega_{TO}=85.4\,\mathrm{cm}^{-1}$, $\gamma_{TO}=4\,\mathrm{cm}^{-1}$, $b=1000\ \mathrm{cm}^{-2}$, $\omega_A=57\,\mathrm{cm}^{-1}$, and $\gamma_A=0.001\,\mathrm{cm}^{-1}$. These values are chosen to give a maximum in $\gamma_\pi(q)$ around $q=755\,\mathrm{cm}^{-1}$ and should be considered only as an indication to describe the phonon self-energy. Thus, the higher damping in the case of the polariton compared to Raman measurements could then be satisfactorily explained. It indicates an important interaction between the polariton and low-frequency excitations, probably in the form of acoustic modes. More data as a function of q and temperature are needed to determine the exact frequency dependence of the phonon self-energy.

V. CONCLUSIONS

The results of a forward, nondegenerate, four-wave-mixing investigation of the A_1(TO) soft mode as function of temperature in the range $10\ \mathrm{K}<T<T_c$ are presented. Interaction with the relaxation mode and low-frequency excitations is inferred. Currently, third-order optical susceptibility measurements as a function of the polariton wave vector and temperature are being carried out. Coupled with infrared and Raman data, they should result in a better understanding of the critical dynamics in such systems.

ACKNOWLEDGMENTS

The research performed at l'Université de Sherbrooke was supported by the Medical Research Council of Canada, the Center of Excellence in Molecular and Interfacial Dynamic, and by le Fonds Pour la Formation des Chercheurs et l'Aide à la Recherche. Research performed at the Oak Ridge National Laboratory, Solid State Division, is supported by the Division of Materials Sciences, U.S. Department of Energy, under Contract No. DE-AC05-84OR21400 with Martin Marietta Systems, Inc.

[1]A. D. Bruce and R. A. Cowley, Adv. Phys. **29**, 1 (1980).
[2]B. I. Halperin and C. M. Varma, Phys. Rev. B **14**, 4030 (1976).
[3]S. M. Shapiro, J. D. Axe, G. Shirane, and T. Riste, Phys. Rev. B **6**, 4332 (1972).
[4]E. Lee, L. L. Chase, and L. A. Boatner, Phys. Rev. B **31**, 1438 (1985).
[5]M. D. Fontana, A. Ridah, G. E. Kugel, and C. Carabatos-Nedelec, J. Phys. C **21**, 5853 (1988).
[6]M. D. Fontana, E. Bouziane, and G. E. Kugel, J. Phys.: Condens. Matter **2**, 8681 (1990).
[7]R. L. Prater, L. L. Chase, and L. A. Boatner, Phys. Rev. B **23**, 221 (1981).
[8]Y. Yan and K. A. Nelson, J. Chem. Phys. **87**, 6240 (1987).
[9]J. Etchepare, G. Grillon, A. Antonetti, J. C. Loulerge, M. D. Fontana, and G. E. Kugel, Phys. Rev. B **41**, 12 362 (1990).
[10]J. Etchepare, G. Grillon, J. P. Chambaret, G. Hamoniaux, and A. Orszag, Opt. Commun. **63**, 329 (1987).
[11]I. Thomazeau, J. Etchepare, G. Grillon, G. Hamoniaux, and A. Orszag, Opt. Commun. **55**, 442 (1985).
[12]A. Laubereau and W. Kaiser, Rev. Mod. Phys. **50**, 607 (1978).
[13]H. J. Eichler, P. Günter, and D. W. Pohl, *Laser-Induced Dynamic Gratings* (Springer-Verlag, Berlin, 1986).
[14]G. M. Gale, F. Vallée, and C. Flytzanis, Phys. Rev. Lett. **57**, 1867 (1986).
[15]H. J. Benson and D. L. Mills, Phys. Rev. B **1**, 4835 (1970).
[16]G. E. Kugel, M. D. Fontana, and W. Kress, Phys. Rev. B **35**, 813 (1987).
[17]D. Rytz, M. D. Fontana, J. L. Servoin, and F. Gervais, Phys. Rev. B **28**, 6014 (1983).
[18]S. Ushioda and J. D. McMullen, Solid State Commun. **11**, 299 (1972).
[19]S. Ushioda, J. D. McMullen, and M. J. Delaney, Phys. Rev. B **8**, 4634 (1973).
[20]A. S. Barker, Phys. Rev. **165**, 917 (1968).
[21]A. S. Barker and J. J. Hopfield, Phys. Rev. **135**, A1732 (1964).